JOURNAL OF SOLID STATE CHEMISTRY 111, 390–396 (1994)

NH_4FePO_4F: Structural Study and Magnetic Properties

Th. Loiseau,* Y. Calage,*,† P. Lacorre,* and G. Férey*,[1]

*Laboratoire des Fluorures, URA CNRS 449, and †Equipe de Physique de l'Etat Condensé, URA CNRS 807, Faculté des Sciences, Université du Maine, Avenue Olivier Messiaen, 72017 Le Mans Cedex, France

Received June 14, 1993; accepted November 5, 1993

Hitherto unknown NH_4FePO_4F has been isolated by low-temperature hydrothermal synthesis. It is orthorhombic and acentric (space group $Pna2_1$ (No. 33); a = 12.993(3) Å, b = 6.468(1) Å, c = 10.640(3) Å, V = 894.2(6) Å^3, Z = 8). This compound belongs to the $KTiOPO_4$ (KTP) structure type, with a strict O–F ordering, the Ti–O short bond in KTP being replaced by a Fe–F bonding. The two iron sites, clearly evidenced by Mössbauer spectroscopy, correspond to two different local situations with 2 F^- in *cis* position for Fe(1) and in *trans* position for Fe(2). With such a configuration, the main magnetic coupling probably occurs within the chains of octahedra via Fe–F–Fe superexchange interactions only, like in $AFeF_5$ and A_2FeF_5 compounds in which the Néel temperature is close to 10 K. However, the high magnetic transition temperature of NH_4FePO_4F (45(1) K) shows that the influence of super-superexchange coupling is rather important in this compound.

INTRODUCTION

After the discovery of cloverite by Estermann *et al.* (1 and references therein), we have undertaken a general study of the conditions of formation under hydrothermal conditions of oxyfluorinated microporous compounds within the systems AF–M_2O_3–P_2O_5–amine (A = H^+, NH_4^+; M = Al, Ga, 3d transition metal) (2–8). For instance, when hexamethylenetetramine (HMTA) is used with Al_2O_3 and Ga_2O_3, microporous compounds with formulation $NH_4MPO_4F_y(OH)_{1-y}$ (y_{Al} = 0.5; y_{Ga} = 0.0) are obtained, the structures of which have been determined (5, 6). The comparison with systems containing 3d transition metals was interesting since, until now, only small amounts of transition metals have been introduced in the diamagnetic matrix of AlPO and GaPO compounds. This paper reports our results in the system NH_4F–Fe_2O_3–P_2O_5–HMTA. Nonmicroporous NH_4FePO_4F is obtained, with a structure different from that of the aluminum and gallium microporous compounds. Its noncentric structure, isotypic with the $KTiOPO_4$ structure (hereafter denoted KTP) (9) and $KFePO_4F$ (11), is described here, with a magnetic susceptibility and Mössbauer study, which evidences the role of super-superexchange magnetic interactions for the onset of the antiferromagnetic ordering of this compound.

[1] To whom correspondence should be addressed.

EXPERIMENTAL

The title compound was obtained as pale yellow single crystals by hydrothermal synthesis under autogeneous pressure at 490 K for 36 hr from a (1 : 1 : 2 : 0.75 : 60) mixture of $Fe(NO_3)_2$, $9H_2O$, P_2O_5, NH_4F, hexamethylenetetramine, and H_2O.

One crystal (0.076 × 0.076 × 0.152 mm), whose quality was checked from Laue photographs, was selected for the structural study. The details of the data collection on the diffractometer Siemens AED 2 are summarized in Table 1.

TABLE 1
Details of the X-Ray Data Collection of NH_4FePO_4F

Determination of cell parameters	32 reflections ($28° \le 2\theta \le 32°$)
Space group	$Pna2_1$ (No. 33)
Cell dimensions	a = 12.993(3) Å
	b = 6.468(1) Å
	c = 10.640(3) Å
Volume/Z	V = 894.2(6) Å^3/Z = 8
Wavelength	0.71069 Å (Mo$K\alpha$)
Scan mode	ω-2θ
Step scan	$35 \le N \le 42$, every 0.035° and 4 sec
Aperture	3 × 3 mm^2
Crystal dimensions	0.076 × 0.076 × 0.152 mm^3
Crystal faces	± (011, 01-1, -30-1, -301)
Absorption correction	Gaussian method
Transmission factors	A_{max} = 0.800; A_{min} = 0.722
Absorption coefficient	μ = 36.6 cm^{-1}
Angular range of data collection	$2\theta \le 70°$
Range of measured h,k,l	$-18 \le h \le 18$; $-10 \le k \le 10$; $0 \le l \le 17$
Standard reflections (3)	(008), (800), (040)
Measured every	60 mn
Maximum intensity variation	3.4%
Measured reflections	4531
Independent ref. ($\|F\|>6\sigma\|F\|$)	2194
Number of refined parameters	172
Secondary extinction factor	0.98(2) × 10^{-7}
Weighting scheme	$1.665/(\sigma^2(F) + 0.00005\,F^2)$
Final Fourier residuals	−0.74 to 0.87 e^- · Å^{-3}
R/R_w	0.024/0.023

0022-4596/94 $6.00

Magnetic susceptibility was measured between 4.2 and 300 K by the Faraday method. Transmission Mössbauer experiments were carried out over the same temperature range, using a spectrometer with a constant acceleration mode and with a ^{57}Co source diffused into a rhodium matrix. The spectra were recorded on powdered samples with 5 mg of iron per square centimeter. The fit to the data was realized with the program MOSFIT (10). The value of the temperature of magnetic order was deduced from the thermal evolution of Mössbauer spectra.

STRUCTURE REFINEMENT AND DESCRIPTION OF THE STRUCTURE

The structure was solved by isotypy with $KFePO_4F$ (11) using the program SHELX-76 (12). Atomic diffusion factors and anomalous diffusion coefficients were taken from (13). The refinement of the position parameters of nonhydrogen atoms and of isotropic thermal motions lowers R to 0.051. Further refinements with anisotropic thermal parameters give $R = 0.038$ and $R_w = 0.040$. Fourier difference syntheses clearly show at this stage the positions of hydrogens of ammonium groups; they were included in the refinement, with a N–H distance constraint and isotropic thermal parameters. The final R of this enantiomer is 0.024 ($R_w = 0.023$). Tables 2 and 3 provide the final positional and thermal parameters and the corresponding characteristic distances and angles. A list of structure factors can be obtained upon request to the

TABLE 2
Atomic Coordinates and Isotropic Thermal Parameters[a] of NH_4FePO_4F

Atom	x/a	y/b	z/c	B (Å²)
Fe(1)	3868(1)	4911(2)	0007(3)	0.50(1)
Fe(2)	2471(1)	2530(b)	2508(*)	0.50(1)
P(1)	5015(2)	3289(1)	2498(3)	0.45(2)
P(2)	1841(1)	4994(3)	5035(4)	0.51(2)
F(1)	2748(4)	4717(8)	1298(5)	0.9(2)
F(2)	2279(4)	0327(9)	3801(5)	0.8(2)
O(1)	4867(5)	4729(11)	1355(5)	0.8(2)
O(2)	5168(5)	4686(11)	3659(5)	0.9(2)
O(3)	4037(3)	2024(7)	2694(6)	0.7(2)
O(4)	5964(3)	1893(7)	2304(6)	0.6(2)
O(5)	1164(4)	3098(6)	5320(5)	0.6(2)
O(6)	1166(5)	6904(7)	4756(6)	1.1(2)
O(7)	2538(4)	5487(11)	6163(6)	0.9(2)
O(8)	2552(4)	4570(11)	3889(5)	0.8(2)
N(1)	3897(4)	7825(6)	3131(5)	1.9(2)
N(2)	0996(3)	6780(7)	0646(5)	1.8(2)
H(1)	393(5)	910(3)	327(7)	4(1)
H(2)	390(5)	761(11)	235(2)	4(1)
H(3)	335(3)	733(10)	344(6)	4(1)
H(4)	441(3)	724(10)	346(6)	4(1)
H(5)	132(5)	672(11)	000(3)	4(1)
H(6)	117(5)	584(8)	110(6)	4(1)
H(7)	039(1)	666(11)	050(7)	4(1)
H(8)	110(5)	785(6)	099(6)	4(1)

Note. Atomic coordinates are multiplied by 10^4 except those of H ($\times 10^3$).

[a] The list of U_{ij} can be obtained upon request.

[b] Fixed.

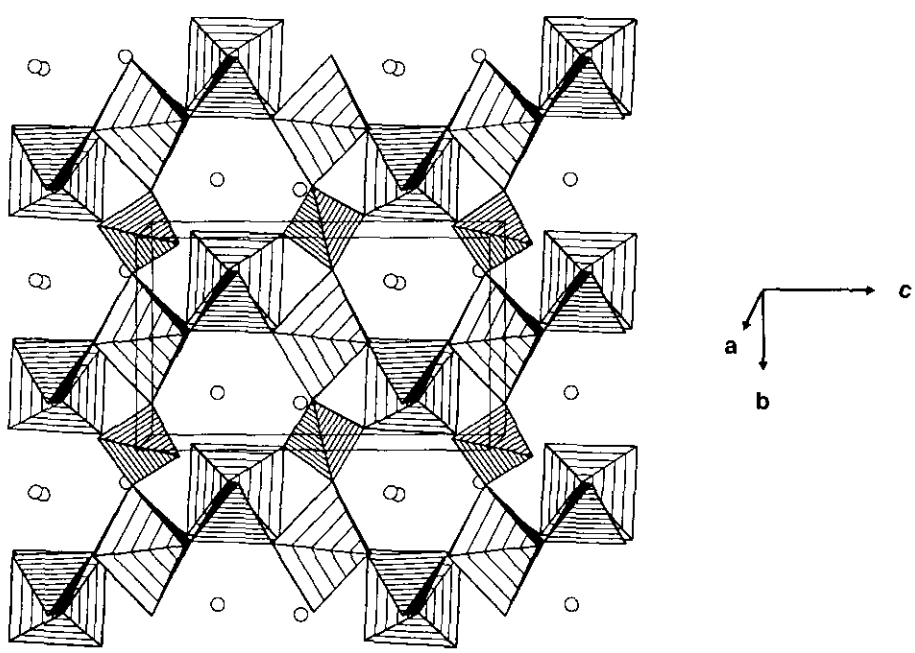

FIG. 1. Perspective view of NH_4FePO_4F close to [100]; slightly hatched octahedra are occupied by Fe(1) and Fe(2) and heavily hatched tetrahedra by P(1) and P(2). Circles correspond to fluoride ions.

TABLE 3
Characteristic Distances (Å) and Angles (°) in Iron and Phosphorus Polyhedra in NH_4FePO_4F

Fe(1) octahedron

Fe(1)	O(2)	O(1)	O(6)	F(2)	F(1)	O(5)
O(2)	1.922(4)	2.894(4)	2.812(4)	2.747(4)	3.920(5)	2.836(4)
O(1)	97.1(4)	1.938(4)	2.835(3)	3.913(5)	2.754(5)	2.785(4)
O(6)	92.7(3)	93.2(3)	1.964(2)	2.833(3)	2.827(4))	4.051(4)
F(2)	89.3(4)	171.7(4)	91.7(3)	1.985(5)	2.686(4)	2.815(4)
F(1)	173.1(4)	88.6(4)	90.9(3)	84.6(4)	2.005(5)	2.804(4)
O(5)	89.9(3)	87.4(3)	177.2(3)	87.4(3)	86.4(3)	2.088(2)

⟨Fe(1)–O⟩ = 1.978 Å, ⟨Fe(1)–F⟩ = 1.995 Å

Fe(2) octahedron

Fe(2)	F(1)	O(7)	O(8)	F(2)	O(4)	O(3)
F(1)	1.946(3)	2.765(4)	2.770(2)	3.940(0)	2.757(5)	2.836(4)
O(7)	90.5(3)	1.948(3)	3.924(0)	2.819(2)	2.852(4)	2.798(4)
O(8)	89.8(3)	177.2(0)	1.978(3)	2.769(4)	2.828(4)	2.837(4)
F(2)	176.1(1)	91.2(3)	88.3(3)	1.996(4)	2.948(4)	2.795(5)
O(4)	88.5(4)	92.3(4)	90.5(3)	94.9(3)	2.005(5)	4.075(5)
O(3)	89.8(3)	88.2(4)	89.0(4)	86.8(4)	178.2(4)	2.070(5)

⟨Fe(2)–O⟩ = 2.000 Å, ⟨Fe(2)–F⟩ = 1.971 Å

P(1) tetrahedron

P(1)	O(3)	O(4)	O(2)	O(1)
O(1)	1.526(5)	2.539(5)	2.486(3)	2.501(3)
O(5)	111.7(5)	1.542(%)	2.532(3)	2.533(3)
O(7)	108.2(4)	110.3(3)	1.542(1)	2.483(4)
O(3)	109.1(4)	110.3(4)	107.1(3)	1.544(7)

⟨P(1)–O⟩ = 1.539 Å

P(2) tetrahedron

P(2)	O(7)	O(5)	O(6)	O(8)
O(7)	1.537(4)	2.526(4)	2.502(4)	2.491(4)
O(5)	110.4(4)	1.539(4)	2.534(2)	2.545(4)
O(6)	108.6(4)	110.5(3)	1.544(4)	2.524(4)
O(8)	107.4(4)	110.7(4)	109.1(4)	1.554(4)

⟨P(2)–O⟩ = 1.544 Å

N(1) tetrahedron

N(1)	H(1)	H(2)	H(4)	H(3)
H(1)	0.84(1)	1.37(1)	1.37(1)	1.38(1)
H(2)	109.6(6)	0.84(1)	1.37(1)	1.37(1)
H(4)	109.1(6)	109.4(8)	0.84(1)	1.38(1)
H(3)	110.3(7)	108.9(6)	109.5(7)	0.84(1)

⟨N(1)–H⟩ = 0.84 Å, constrained

N(2) tetrahedron

N(2)	H(8)	H(7)	H(5)	H(6)
H(8)	0.80(1)	1.31(1)	1.31(1)	1.31(1)
H(7)	109.8(7)	0.81(1)	1.32(1)	1.31(1))
H(5)	110.2(7)	109.9(8)	0.81(1)	1.32(1)
H(6)	109.4(5)	108.4(8)	109.1(7)	0.81(1)

⟨N(2)–H⟩ = 0.81 Å, constrained

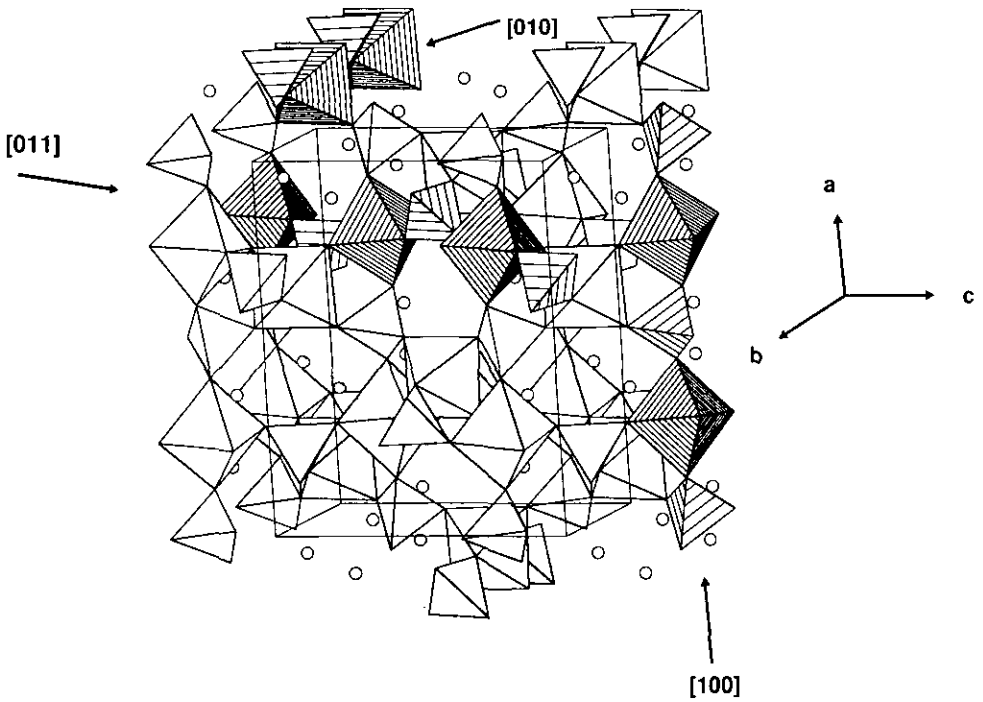

FIG. 2. Perspective view of NH_4FePO_4F; hatched polyhedra belong to the rods developing along [100], [010], and [011]. Circles correspond to F^-.

authors.[2] The crystal chemistry of NH_4FePO_4F could be described in the centric space group *Pnna*, but this group would induce a supplementary *hk0* condition ($h + k = 2n$) which is not observed on the data.

The main feature in this structure is the strict anionic O–F ordering. F^- ions occupy the sites of the oxygen strongly bounded to Ti in KTP (Ti=O ~ 1.72 Å), but this time the Fe–F distances (~1.98 Å) are about the same as the other Fe–O distances. This anionic order clearly differentiates the two iron octahedral sites of the structure. Both surroundings consist of four oxygen and two fluorine atoms, but while around Fe(1), the two F^- are in *cis* position; they are in *trans* situation around Fe(2). This explains, as it will be seen below, the two different contributions observed in the Mössbauer spectra of NH_4FePO_4F. Figures 1 and 2 give two different perspective views of the structure. They show its identity with the structural type KTP, which provides another nice example of rod packing structures as mentioned by O'Keeffe and Andersson (14). These rods are built from chains formed by alternating PO_4 tetrahedra and FeO_4F_2 octahedra, linked by oxygen corners; these chains run along [100], [010], and [011] (Fig. 2). This rod packing leads to six-membered ring channels in which ammonium atoms are located. It also ensures the connection of FeO_4F_2 octahedra via fluorine corners. The resulting zig-zag chains of FeO_4F_2 octahedra (Fig. 3) run along [011] and [0-11], which represent the only two directions within which long-range magnetic superexchange interactions can occur via 180° Fe–F–Fe pathways. From this point of view, NH_4FePO_4F might be considered as a 1D antiferromagnet with exclusively Fe^{3+}–F^-–Fe^{3+} interactions. If that were the case, the expected magnetic ordering temperature would be very low, for instance close to that observed in 1D antiferromagnetic fluorides (hydrated or not) $AFeF_5$ (A = alcaline earth ions) or A_2FeF_5 (A =

[2] See NAPS Document 00000 for 00 pages of supplementary material. Order from ASIS/NAPS, Microfiche Publications, P.O. Box 3513, Grand Central Station, New York, NY 10163. Remit in advance $4.00 for microfiche copy or for photocopy, $7.75 for up to 20 pages plus $0.30 for each additional page. All orders must be prepaid. Institutions and organizations may order by purchase order. However, there is a billing and handling charge for this service of $15.00. Foreign orders add $4.50 for postage and handling, for the first 20 pages, $1.00 for each additional 10 pages of material, and $1.50 for postage of any microfiche orders.

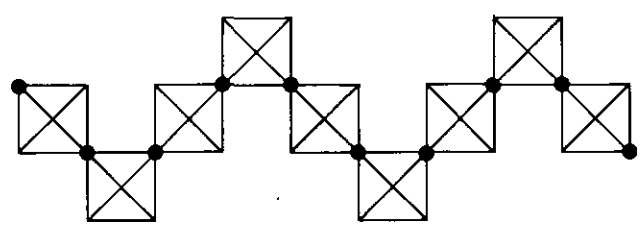

FIG. 3. Idealized zig-zag chains of FeO_4F_2 octahedra along [011]; black circles, F^-.

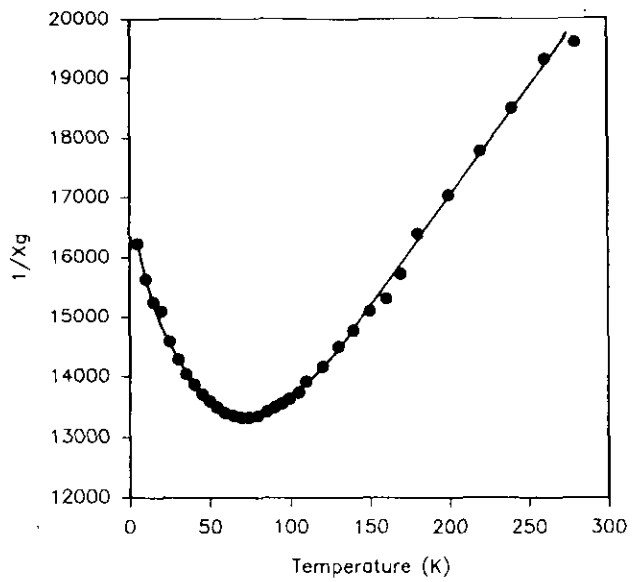

FIG. 4. Thermal evolution of the inverse magnetic susceptibility curve of NH_4FePO_4F.

alcaline ion), which order around 10 K (15, 16, and references therein).

MAGNETIC PROPERTIES

The inverse magnetic susceptibility (Fig. 4) varies linearly only in the range 200–300 K. The experimental molar Curie constant (C_M = 4.95) is therefore approximative since high-temperature experiments would be needed to have an accurate value of C_M closer to the theoretical value (C_{th} = 4.375). The negative value of θ_p (−227(10) K) indicates the presence of strong antiferromagnetic interactions. The antiferromagnetic ordering temperature value (45 K from Mössbauer spectroscopy) does not correspond to the minimum of $\chi^{-1}(T)$ curve: 76(4) K.

The spectra recorded at 300 and 77 K (Fig. 5) indicate the presence of pure electric hyperfine interactions. The

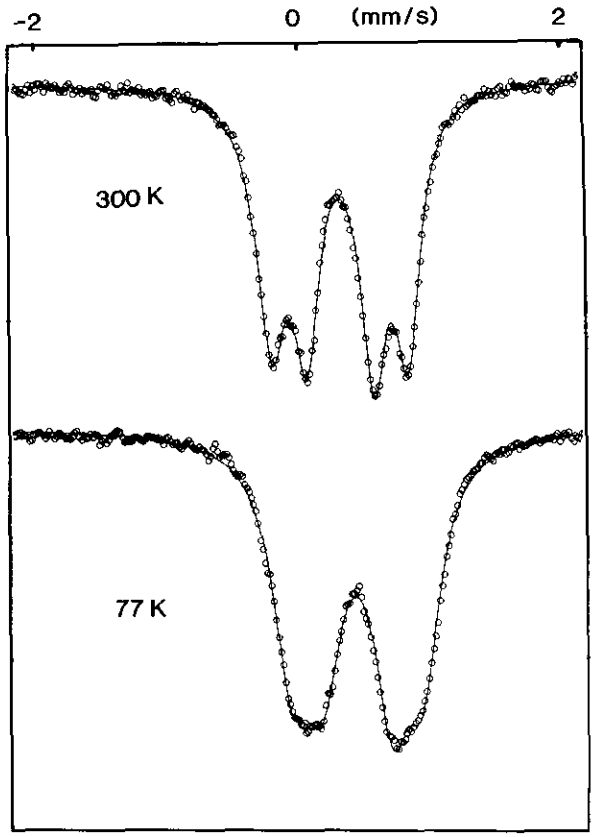

FIG. 5. Paramagnetic Mössbauer spectra of NH_4FePO_4F.

paramagnetic spectra exhibit, especially at 300 K, two well-resolved quadrupole doublets, corresponding to the two different octahedral surroundings of Fe(1) and Fe(2). Their isomer shifts (I.S.) (Table 4) are quasi-identical (0.44 mm/s) but quadrupole splitting values are very different (Q.S. = 0.5 and 1.0 mm/s, respectively) and reflect the different repartition of anions around each octahedral site, but we were unable to attribute the experimental values to the corresponding iron sites. However, all the hyperfine

TABLE 4
Refined Mössbauer Parameters of NH_4FePO_4F

	Site 1[a]				Site 2[a]				
T (K)	I.S. (mm/sec)	QS/2ε (mm/sec)	Γ (mm/sec)	H_{hf} (kOe)	I.S. (mm/sec)	QS/2ε (mm/sec)	Γ (mm/sec)	H_{hf} (kOe)	S_1/S_2
300	0.445	0.505	0.25	—	0.442	1.03	0.25	—	1.0
77	0.54	0.52	0.34	—	0.54	0.99	0.32	—	1.1
30	0.55	0.16	0.42	409	0.55	−0.41	0.42	407	1.1
4.2	0.55	0.15	0.32	506	0.55	−0.44	0.34	501	1.0

Note. I.S., isomer shift (mm · s^{-1}) with reference to metallic iron at 300 K (e.s.d. are 0.01 except at 300 K, where e.s.d. are 0.004); Γ, linewidth at half-height (mm · s^{-1}) of the Lorentzian peak (e.s.d. are 0.05); QS/2ε, quadrupolar splitting/shift (mm · s^{-1}) (e.s.d. are 0.01 except at 300 K, where e.s.d. are 0.004); H_{hf}, hyperfine field (kOe); (e.s.d. are 2 at 4.2 K and 5 at 30 K.

[a] Labels 1 and 2 are only used to differentiate the sites. There is no direct relation with the crystallographic sites Fe(1) and Fe(2).

parameters are characteristic for high-spin Fe^{3+} (17). Moreover, the fitted relative areas of the doublets lead to a S_1/S_2 ratio equal to 1, in agreement with the crystal structure.

The magnetic spectrum at 4.2 K (Fig. 6) exhibits two resolved sextets whose relative area ratio is close to 1 : 1. The corresponding hyperfine parameters give two hyperfine field values of ca. 510 kOe, already observed in other Fe^{3+} fluorides (18). The thermal evolution of H_f vs T, given in Fig. 7, provides the value of T_N: 45(2) K.

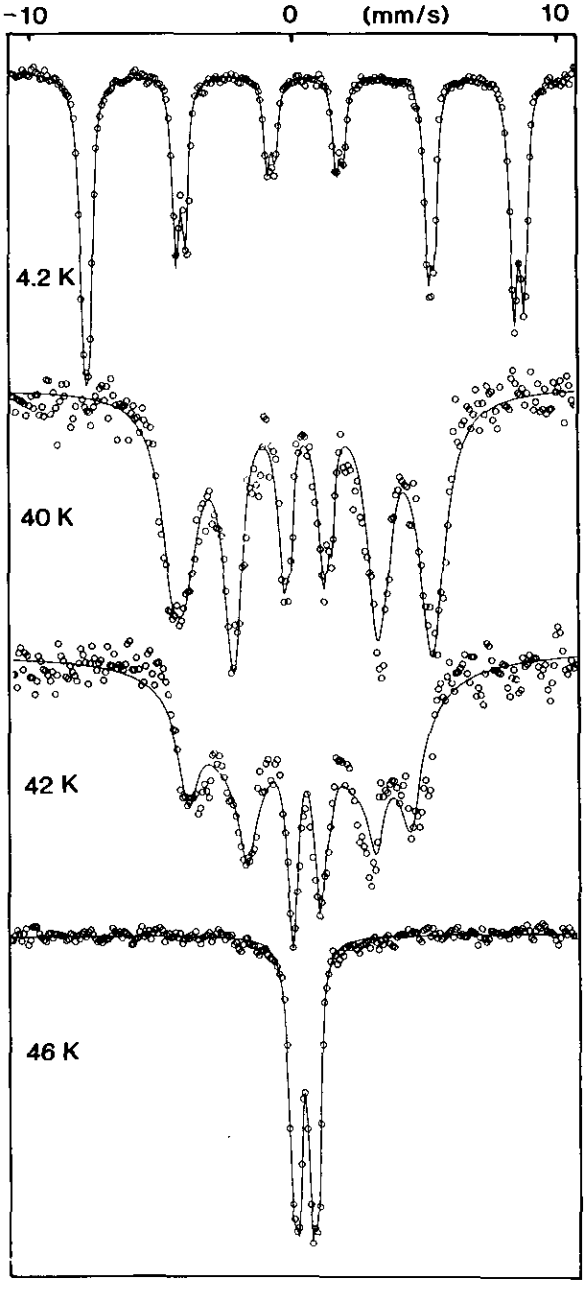

FIG. 6. Thermal evolution of the Mössbauer spectra in the magnetic state.

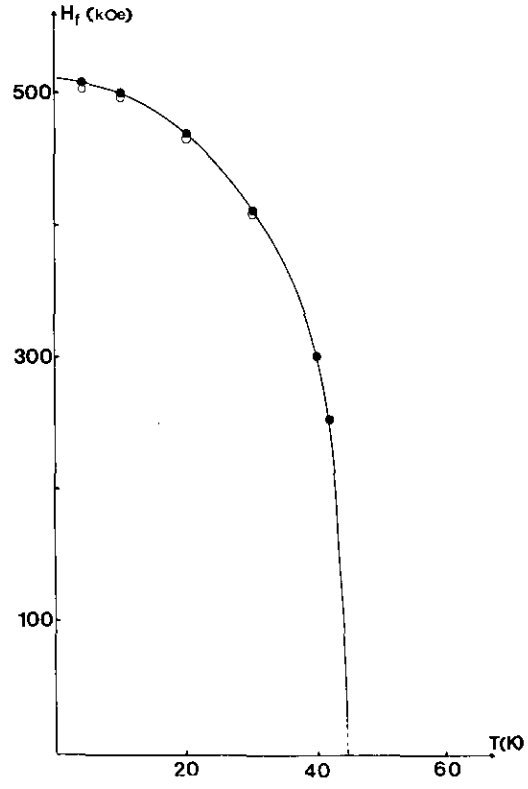

FIG. 7. Thermal variation of the magnetic hyperfine fields of NH_4FePO_4F.

These values are somewhat surprising when compared to the data of 1D antiferromagnetic fluorides in which T_N is always very close to 10 K and the hyperfine field at 4.2 K to 430 kOe. This relatively high 3D magnetic ordering temperature is to be compared to that observed in other iron phosphates, where Néel temperatures, as high as 40 K, were observed despite the absence of any direct superexchange interaction (see, for instance, Refs. (19) and (20) and references therein). This is most probably due to the existence of nonnegligible Fe–O–O–Fe super-superexchange interactions, although phosphate groups must be taken into account to explain them. The determination of the magnetic structure, currently in progress, will give more information on the characteristics of each magnetic site and on the coupling modes in the structure.

ACKNOWLEDGMENTS

The authors are very indebted to Professor M. Leblanc and Dr. R. Retoux (Université du Maine) for the collection of X-ray data.

REFERENCES

1. M. Estermann, L. B. McCusker, C. Baerlocher, A. Merrouche, and H. Kessler, *Nature* **352,** 320 (1991).
2. D. Riou, T. Loiseau, and G. Férey, *J. Solid State Chem.* **99,** 414 (1992).

3. T. Loiseau and G. Férey, *J. Chem. Soc. Chem. Commun.* 1197 (1992).
4. D. Riou, T. Loiseau, and G. Férey, *J. Solid State Chem.* **101,** (1992).
5. G. Férey, T. Loiseau, F. Taulelle, and P. Lacorre, *J. Solid State Chem.* **105,** 179 (1993).
6. F. Taulelle, T. Loiseau, J. Maquet, J. Livage, and G. Férey, *J. Solid State Chem.* **105,** 191 (1993).
7. D. Riou, T. Loiseau, and G. Férey, *Acta Crystallogr. Sect. C* **49,** 1237 (1993).
8. T. Loiseau and G. Férey, *Eur. J. Solid State Inorg. Chem.* **30,** 369 (1993).
9. I. Tordjman, R. Masse, and J. C. Guitel, *Z. Kristallogr.* **139,** 103 (1974).
10. J. Teillet and F. Varret, Mosfit Program, unpublished.
11. E. L. Belokovena, O. V. Yakubovitch, V. G. Tsirel'son, and V. S. Urusov, *Izv. Akad. Nauk. SSSR Neorg. Mater.* **26**(3), 595 (1990).
12. G. M. Sheldrick, *in* "Crystallographic Computing 3" (G. M. Sheldrick, C. Kruger, and R. Goddard, Eds.) p. 175. Oxford Univ. Press, London (1985).
13. Th. Hahn (Ed.), "International Tables of Crystallography." Academic Kluwer Press, Dortrecht, The Netherlands, 1987.
14. M. O'Keeffe and S. Andersson, *Acta Crystallogr. Sect. A* **33,** 914 (1977).
15. Y. Laligant, J. Pannetier, and G. Férey, *J. Solid State Chem.* **66,** 242 (1987).
16. J. L. Fourquet, R. De Pape, J. Teillet, F. Varret, and G. C. Papaefthymiou, *J. Magn. Magn. Mater.* **27,** 209 (1982).
17. Y. Calage, M. C. Moron, J. L. Fourquet, and F. Palacio, *J. Magn. Magn. Mat.* **98,** 79 (1991).
18. Y. Calage, M. Zemirli, J. M. Greneche, F. Varret, and G. Férey, *J. Solid State Chem.* **69,** 197 (1987).
19. N. Fanjat and J. L. Soubeyroux, *J. Magn. Magn. Mat.* **104,** 933 (1992).
20. N. Fanjat and G. Lucazeau, *J. Phys. Chem. Solids* **54,** 187 (1993).